

# Electrical properties and microstructure of phase combination in BaTiO<sub>3</sub>-based Ceramics

N Funsueb<sup>1,2</sup>, A Limpichaipanit<sup>1</sup>, A Ngamjarrojana<sup>1,\*</sup>

<sup>1</sup> Department of Physics and Materials Science, Faculty of Science, Chiang Mai University, Chiang Mai, 50200, Thailand

<sup>2</sup> PhD's Degree Program in Applied Physics, Faculty of Science, Chiang Mai University, Chiang Mai, 50200, Thailand

\*E-mail: ngamjarrojana@yahoo.com

**Abstract.** Perovskite barium titanate (BaTiO<sub>3</sub>) ceramics are widely used in electronics industries such as capacitors, sensors and actuators. BaTiO<sub>3</sub>-based ceramics have good dielectric, ferroelectric and piezoelectric properties. BaTiO<sub>3</sub> powder was fabricated by mixed-oxide method via a vibro-milling technique. The pellets were then placed in a high purity alumina crucible in air and sintered at 1375 °C for 1, 2, 4, 6 and 8h. X-ray diffraction technique was used to investigate phase formation of BaTiO<sub>3</sub> ceramics. Grain size was measured by scanning electron microscopy (SEM). The computer-controlled dielectric measurement system consisted of a high precision LCR-meter. Electric field induced polarization was measured by Sawyer-Tower circuit. In this work, the effect of phase combination in BaTiO<sub>3</sub> ceramics on electrical properties (dielectric and electric field induced polarization) and microstructure was investigated.

## 1. Introduction

Barium titanate or BaTiO<sub>3</sub> is one of the most basic and widely ferroelectric oxide materials with a perovskite-type crystalline structure that has many excellent functional properties such as dielectric, ferroelectric, piezoelectric and electro-optic properties. Therefore, they have been widely used in various electronic devices. BaTiO<sub>3</sub> is of interest in the context of ceramic capacitors, sensors, transducers and actuators [1]. Phase transition of BaTiO<sub>3</sub> at the Curie temperature ( $T_c$ ) is 130 °C approximately. The phase transition in order of cooling temperature is cubic-to-tetragonal, tetragonal-to-orthorhombic, and orthorhombic-to-rhombohedral where the temperature above the Curie point refers to the crystal symmetry (cubic phase) with paraelectric phase [2]. BaTiO<sub>3</sub> has a remnant polarization of 0.30 C/m<sup>2</sup>, coercive field of 0.35 kV/mm, piezoelectric coefficient of 191 pC/N and high electromechanical coupling factor of 0.5. Recently, BaTiO<sub>3</sub> is modified for actuator application such as barium zirconate titanate BZT and barium calcium titanate BCT and BaTiO<sub>3</sub> doped [3].

In this work, BaTiO<sub>3</sub> ceramics were sintered at 1375 °C for 1, 2, 4, 6 and 8h. X-ray diffraction technique was used to investigate phase formation of BaTiO<sub>3</sub> ceramics. The computer-controlled dielectric measurement system consisted of a high precision LCR-meter was used to measure the dielectric constant. Microstructure was investigated by SEM. Electric field induced polarization measure by Sawyer-Tower circuit with electric field strength at 20 kV/cm. The phase combination-property relation in terms of electrical and microstructure properties will be discussed.

## 2. Experimental procedure

Barium titanate powder was prepared from mixed-oxide method (mixture of  $\text{BaCO}_3$  and  $\text{TiO}_2$ ). All powders were weighed, mixed and further milled by vibro-milling (McCrone Micronizing Mill) for 30 minutes with a corundum cylindrical media in ethanol. After drying at  $120^\circ\text{C}$  for 24 h, the mixture of oxides was calcined at  $1250^\circ\text{C}$  for 4 h in air. Green pellets of 10.0 mm diameter were prepared using uniaxial-pressure of 150 MPa. The pellets were then placed in a high purity alumina crucible in air and sintered at  $1375^\circ\text{C}$  for 1, 2, 4, 6 and 8h. The sintered samples were polished, cleaned and screen printed with silver electrodes. The XRD patterns at room temperature were recorded by X-ray diffraction (SMARTLAB X-ray diffractometer). The  $\text{CuK}_\alpha$  radiation was used as X-ray source. Scanning electron microscopy (SEM) was used to determine grain size by fracture surface. The dielectric properties of the sintered ceramics were studied as a function of temperature with an automated dielectric constant and dielectric loss measurement system. The computer-controlled dielectric measurement system consisted of a high precision LCR-meter, a temperature chamber and a computer system. The dielectric constant was determined over the temperature range of  $100\text{-}200^\circ\text{C}$ . Electric field induced polarization was measured by using Sawyer-Tower circuit with electric field strengths at 20 kV/cm.

## 3. Result and discussion

### 3.1. X-ray diffraction pattern (XRD)

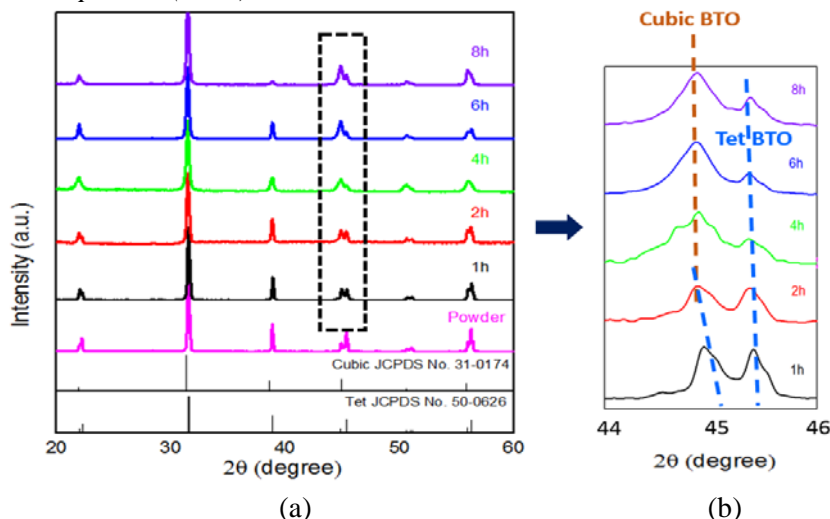


Figure 1. Shows (a) XRD pattern of  $\text{BaTiO}_3$  powder and  $\text{BaTiO}_3$  ceramics and (b) peak split at  $2\theta = 44 - 46$

Figure 1 (a) shows that the XRD patterns of  $\text{BaTiO}_3$  powder and ceramics revealed perovskite structure for all compositions. The powder after calcination represented tetragonal phase as confirmed by JCPDS no. 50-0626 but after sintering it was found that when increasing soaking time phase combination changed from pure tetragonal phase to mixed tetragonal and cubic phase as confirmed by JCPDS no. 31-0174. Figure 1 (b) shows phase combination from the peaks of  $2\theta = 44 - 46$  after curve fitting and the calculated area under curve was used to find the phase ratio is shown in Table 1. From the result, it was found that the percentage of cubic phase increased with the increasing soaking time [4, 5]. The phase combination affected electrical and ferroelectric properties which will be discussed in the next part.

### 3.2. Microstructure

Generally, microstructure and grain size are a function of soaking time (grain growth process) [6, 7]. Figure 2 (a) shows a scanning electron microscopy (SEM) image of  $\text{BaTiO}_3$  sintered at  $1375^\circ\text{C}$  for 2h. Average grain size of all sample is shown in Figure 2 (b) and Table 1. The result shows that grain size

increased with increasing soaking time. The biggest grain size at soaking time of 8h was 9.58  $\mu\text{m}$ . The ratio of phase combination did not affect grain growth mechanism. From the result, it was found that grain size increased resulting from the increased soaking time.

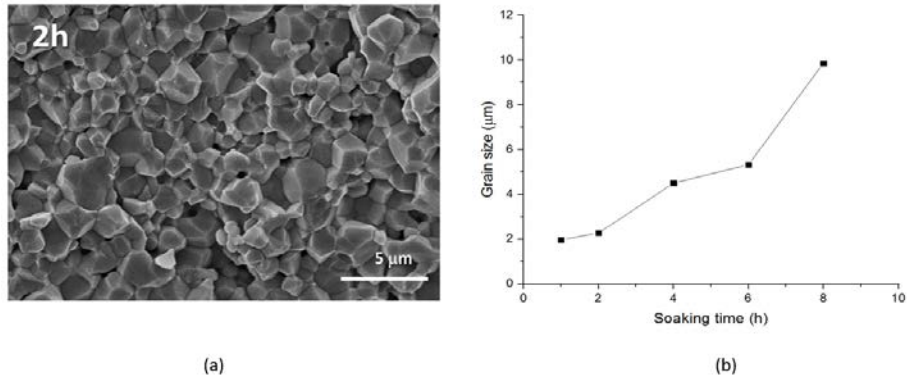


Figure 2. Shows (a) sample grain sizes of BaTiO<sub>3</sub> ceramics (sinter at 1375 °C for 2h) and (b) graph grain size versus soaking time

### 3.3. Dielectric properties

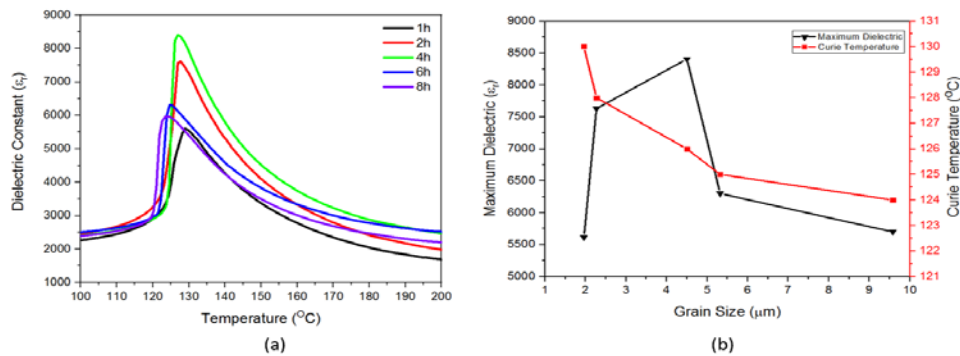


Figure 3. Shows (a) graph of dielectric constant with various soaking times (b) graph grain size with various maximum dielectric and Curie temperature

Figure 3 (a) shows dielectric constant ( $\epsilon_r$ ) of BaTiO<sub>3</sub> sintered at 1375 °C for 1, 2, 4, 6 and 8h as a function of temperature at the frequency of 1 kHz. Curie temperature and maximum dielectric value are calculated in Table 1. The graph shows peak at soaking times of 1, 2, 4, and 8h which are characteristic of normal ferroelectric materials. Normally, Curie temperature was around 130 °C but the increase of cubic phase resulted in the decrease of phase transition temperature [8, 9]. Figure 3 (b) graph grain size with various maximum dielectric and Curie temperature it was found that the optimization maximum dielectric value of the sample sintered at 1375 °C for 4 h was 8406 and Curie temperature decreased with increased grain size.

### 3.4. Electric field induced polarization

Figure 4 shows polarization hysteresis loop versus electric field of BaTiO<sub>3</sub> sintered at 1375 °C for 1, 2, 4, 6 and 8h. The polarization values are calculated and shown in Table 1. Polarization versus electric field hysteresis loops of BaTiO<sub>3</sub> ceramics was plotted at the maximum electric field at 20 kV/cm and the frequency of 5 Hz. The values of remnant polarization and coercive field decreased with increasing soaking time but spontaneous polarization value increased with increasing soaking time. The shape of polarization hysteresis loop change to slim loop after increasing soaking time resulting from behavior of combination phase (cubic and tetragonal phase) [10, 11]. The values of remnant polarization, coercive field and spontaneous polarization depend on grain size and shape of polarization hysteresis loop depend on cubic phase in combination phase.

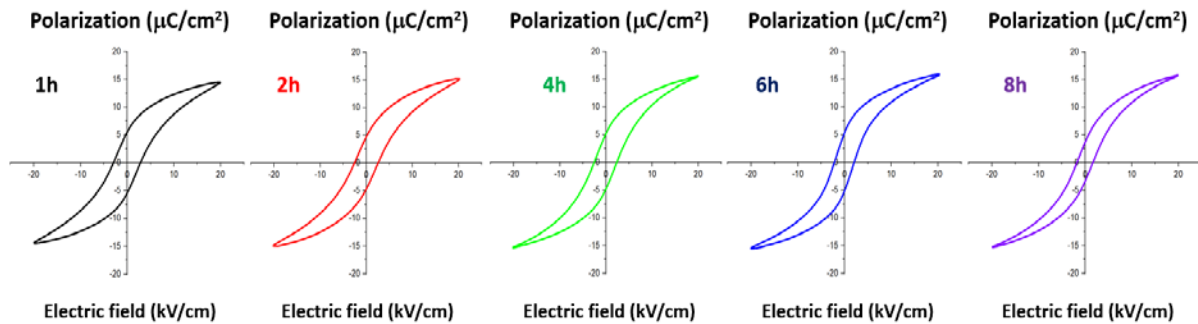


Figure 4. Graph of electric field induced polarization at 20 kV/cm.

Table 1. Shows phase ratio, grain size,  $T_c$ , dielectric properties and ferroelectric properties.

Soaking time	Phase ratio	Grain size	$T_c$	Dielectric Constant	Dielectric Loss	Remnant Polarization	Spontaneous Polarization	Coercive Field
h	%T:%C	$\mu\text{m}$	$^{\circ}\text{C}$	$\epsilon_r$	$\tan\delta$	$\mu\text{C}/\text{cm}^2$	$\mu\text{C}/\text{cm}^2$	kV/cm
1	90.91 : 9.090	$1.96 \pm 0.19$	130	5615	0.01	5.55	14.51	2.84
2	87.35 : 12.65	$2.27 \pm 0.30$	128	7630	0.02	5.11	15.22	2.56
4	71.28 : 28.72	$4.50 \pm 0.88$	126	8406	0.01	4.66	15.57	2.48
6	57.61 : 42.39	$5.32 \pm 1.35$	125	6300	0.02	4.27	15.64	2.08
8	53.85 : 46.15	$9.58 \pm 1.06$	124	5701	0.02	3.59	15.76	1.65

#### 4. Conclusion

In this study,  $\text{BaTiO}_3$  ceramics were successfully prepared by a solid-state mixed oxide technique. The powder after calcination represent pure tetragonal phase confirmed. After sintering, it was found that when increased soaking time resulted in phase combination (cubic and tetragonal phase) in  $\text{BaTiO}_3$  occurred. Grain size increased with increasing soaking time and phase combination did not affect grain growth process. Electrical properties (dielectric and polarization) are according to grain size and phase ratio as the increase of cubic phase resulted in the decrease phase transition point and shape of polarization hysteresis loop changed to slim loop.

#### 5. Acknowledgements

This work was supported by Laser and Applied Optics Research Laboratory, Department of Physics and Materials Science, Faculty of Science, Chiang Mai University. The authors are thankful to Faculty of Science, Graduate School and Chiang Mai University for financial support.

#### References

- [1] Uchino K 2010 *Ferroelectric devices (2<sup>nd</sup> edition)* CRC Press, Boca Raton FL ISBN 978-1-4398-0375-2
- [2] Koruza J, Bell A J, Fromling T, Webber K G and Rodel J 2018 *J Materiomics* **4** 13-26
- [3] Gao J, Xue D, Liu W, Zhou C and Ren X 2017 *Actuators* **6(24)** 1-20
- [4] Zhang Q, Cagin T and Goddard W A 2006 *Proc Natl Acad Sci U S A* **103(40)** 14695-14700
- [5] Wang H and Wu J 2014 *Journal of Alloys and Compounds* **615** 969-974
- [6] Chumprasert L, Limpichaipanit A, Chokethawai K, Ananta S and Ngamjarurojana A 2013 *Ferroelectrics* **457** 16-22
- [7] Wu Y, Zhang J, Tan Y and Zheng P 2016 *Ceramics International* **42** 9815-9820.
- [8] Shin D J, Kim J, Jeong S J and Koh J H 2016 *Materials Research Bulletin* **82** 7-10
- [9] Lu D Y, Cui S Z, Lui Q L and Sun X Y 2016 *Ceramics International* **42** 14364-14373
- [10] He C, Wang Z, Li X, Yang X and Ye Z G 2017 *Acta Materialia* **125** 498-505
- [11] Funsueb N, Ngamjarurojana A, Tunkasiri T and Limpichaipanit A 2018 *Ceramics International* **44** 6343-6353